



# Hard magnetic properties of interstitial compounds $\text{Sm}_3(\text{Fe,Cr})_{29}\text{X}_y$ ( $\text{X}=\text{N}, \text{C}$ )

Yi-Zhong Wang<sup>a,c,\*</sup>, Bo-Ping Hu<sup>a</sup>, Gui-Chuan Liu<sup>a</sup>, Hong-Shuo Li<sup>b</sup>, Xiu-Feng Han<sup>c</sup>,  
Chang-Ping Yang<sup>c</sup>, Jifan Hu<sup>d</sup>

<sup>a</sup>San Huan Research Laboratory, Chinese Academy of Sciences, P.O. Box 603, Beijing 100080, China

<sup>b</sup>School of Physics, The University of New South Wales, Sydney, NSW 2052, Australia

<sup>c</sup>National Magnetism Laboratory, Chinese Academy of Sciences, P.O. Box 603, Beijing 100080, China

<sup>d</sup>Department of Physics, Shandong University, Jinan 250100, China

## Abstract

Interstitial rare-earth iron-rich  $\text{Sm}_3(\text{Fe,Cr})_{29}\text{X}_y$  ( $\text{X}=\text{N}, \text{C}$ ) compounds with the monoclinic  $\text{Nd}_3(\text{Fe,Ti})_{29}$  structure have been successfully synthesized by gas–solid reaction. An intrinsic coercivity  $\mu_{0i}H_c$  of  $\sim 0.80$  T at 293 K has been attained for both the nitride and carbide prepared by ball-milling. The intrinsic coercivity  $\mu_{0i}H_c$  of the nitride powder increases with decreasing average particle size  $d$  and exhibits a maximum at  $d=0.4$   $\mu\text{m}$ , then decreases slowly for smaller  $d$  values. Our results suggest that the coercivity of the  $\text{Sm}_3\text{Fe}_{24}\text{Cr}_5\text{N}_y$  powder is mainly controlled by a nucleation mechanism as observed in the  $\text{Sm}_3(\text{Fe,Ti})_{29}\text{N}_y$  and 2:17:N nitrides. A remanence of  $B_r=0.87$  T has been achieved at 293 K for  $\text{Sm}_3\text{Fe}_{24}\text{Cr}_5\text{N}_y$  which gives an energy product of  $(\text{BH})_{\text{max}}=104.8$   $\text{kJ/m}^3$ . Similar hard magnetic properties were observed for the carbide powder. The temperature coefficient of the remanence of the carbide is worse than that of Nd–Fe–B, although it has a better temperature coefficient of coercivity. Both the nitride and carbide powders have better corrosion resistance than commercial Nd–Fe–B powder. © 1998 Elsevier Science S.A. All rights reserved.

**Keywords:** Permanent magnetic materials; Nitrides; Carbides; Rare-earth iron compounds

## 1. Introduction

The structures of the  $\text{R}_2(\text{Fe}_{0.91}\text{V}_{0.09})_{17}$  ( $\text{R}=\text{Y}, \text{Nd}, \text{Sm}, \text{Gd}$ ) and  $\text{Nd}_2(\text{Fe,Ti})_{19}$  phases, discovered by Shcherbakova et al. [1] and Collocott et al. [2], respectively, were identified as being the monoclinic  $\text{Nd}_3(\text{Fe,Ti})_{29}$  (3:29) structure by Li et al. [3] and Hu and Yelon [4]. Interstitial modification of the 3:29 rare-earth iron-rich compounds,  $\text{R}_3(\text{Fe,M})_{29}\text{X}_y$  ( $\text{M}=\text{Ti,V,Cr,Mn,Mo}$  and  $\text{X}=\text{N}, \text{C}$ ), leads to a similar enhancement of the intrinsic magnetic properties as observed in the 2:17-type compounds. Excellent intrinsic magnetic properties such as high magnetic ordering temperature, high magnetization and strong uniaxial anisotropy are achieved in the 3:29:X compounds with  $\text{R}=\text{Sm}$  [2,5–9]. This enhancement makes  $\text{R}_3(\text{Fe,M})_{29}\text{X}_y$  a potential candidate for use as a permanent magnet material. In the past four years, we have been successful in synthesizing various 3:29-type nitrides and carbides:  $\text{R}_3(\text{Fe,M})_{29}\text{X}_y$  ( $\text{M}=\text{Ti}, \text{V}, \text{Cr}, \text{Mo}$  and  $\text{X}=\text{N}, \text{C}$ ), and we have investigated their intrinsic magnetic properties [5–9] and their extrinsic hard magnetic properties [10–14]. In

this paper we report the results of a study of the extrinsic hard magnetic properties, thermostability and corrosion resistance of the interstitial compounds  $\text{Sm}_3\text{Fe}_{24}\text{Cr}_5\text{X}_y$  ( $\text{X}=\text{N}$  and  $\text{C}$ ).

## 2. Experimental

Ingots with the composition  $\text{Sm}_3\text{Fe}_{24}\text{Cr}_5$  were prepared by argon arc-melting starting elements of at least 99.9% purity. The starting compositions contained 10 wt.% excess Sm in order to compensate for the Sm loss during melting. The arc-melted ingots were wrapped in molybdenum foil, sealed in quartz tubes under an argon atmosphere and annealed at 1273–1323 K for 1–5 days. At the end of the annealing, the ingots were quenched in water. The annealed samples were examined by both x-ray powder diffraction (XRD) and thermomagnetic analysis (TMA). Single phase ingots were ground into fine powder with a grain size of 20–35  $\mu\text{m}$ . The nitrogenation or carbonation was performed by heating the fine powder in nitrogen or acetylene, respectively, at a pressure of 1 atm in the temperature range 773–873 K for 3–4 h. During the

\*Corresponding author.

carbonation process, the sample space was pumped before cooling to avoid the absorption of hydrogen by the sample. The nitride and carbide powders, both of which contained traces of  $\alpha$ -Fe, were then ball-milled in petroleum ether using metal balls of 4–10 mm diameter with a sample-to-ball weight ratio of 1:60. Magnetically aligned cylindrical samples were made by mixing the ball-milled powders with about 50 wt% epoxy resin, and then solidifying the mixture in an applied field of 1.2 T at room temperature. Average particle sizes ( $d$ ) of the ball-milled powders were estimated by optical microscopic observation of the polished end surfaces of the cylinders. After the samples were magnetized at 293 K in open circuit with a pulsed field of  $\sim 4$  T, hysteresis loops were measured using a SQUID magnetometer in the temperature range 1.5–293 K and a vibrating sample magnetometer (VSM) in the temperature range 293–450 K. The demagnetization effect was corrected according to the sample shape. Examination of the corrosion resistance of the nitride and carbide powders was performed under environmental conditions with 87% relative humidity at 297.5 K for 70 days.

### 3. Results and discussion

#### 3.1. Hard magnetic properties at 293 K

The original coarse nitride or carbide powders with particle sizes of 20–35  $\mu\text{m}$  have a very small coercivity but substantial coercivity can be developed by ball-milling [10–14]. Fig. 1 shows the dependence on the average particle size  $d$  of the coercivity  $\mu_{0i}H_c$ , remanence  $B_r$  and energy product  $(BH)_{\text{max}}$ , deduced from the hysteresis loop measurements at 293 K on the  $\text{Sm}_3\text{Fe}_{24}\text{Cr}_5\text{N}_y$  cylindrical samples magnetized using a pulsed field of  $\sim 4$  T prior to measurement. It can be seen that with decreasing  $d$ , first  $\mu_{0i}H_c$ ,  $B_r$  and  $(BH)_{\text{max}}$  increase rapidly then  $B_r$  and  $(BH)_{\text{max}}$  reach maxima at around  $d=2.5$   $\mu\text{m}$  and finally they decrease rapidly for lower  $d$  values, while  $\mu_{0i}H_c$  continuously increases through  $d=2.5$   $\mu\text{m}$  up to  $d=1$   $\mu\text{m}$  and reaches a plateau of 0.75 T between  $d=1.0$   $\mu\text{m}$  and 0.4  $\mu\text{m}$ , before decreasing very gradually. The particle sizes in the range 0.2–25  $\mu\text{m}$  are large enough relative to the critical single-domain diameter  $D_c$  (about 0.1  $\mu\text{m}$ ) for the nitride particles to be multi-domain. Usually, the coercivity of these multi-domain particles increases with decreasing particle size [15], as seen at  $d>1$   $\mu\text{m}$  in Fig. 1. The effect of the ball-milling not only reduces the size of the particles, but also increases the surface defects. The former tends to increase the coercivity, the latter tends to reduce it. The coercivity plateau at  $0.4$   $\mu\text{m}<d<1$   $\mu\text{m}$  is a consequence of the balance between these mechanisms, and the decrease in the coercivity at  $d<0.3$   $\mu\text{m}$  can be attributed to the oxidation of very fine powders. For a magnetizing field of about 4 T, the maximum values of  $\mu_{0i}H_c$ ,  $B_r$  and  $(BH)_{\text{max}}$  at room temperature are 0.75 T,

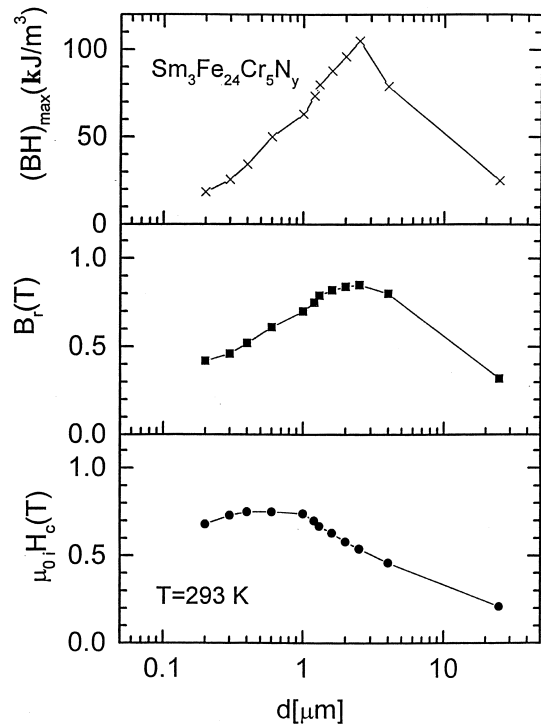


Fig. 1. Variation of the remanence ( $B_r$ ), coercivity ( $\mu_{0i}H_c$ ) and energy product  $(BH)_{\text{max}}$  with average particle size ( $d$ ) of  $\text{Sm}_3\text{Fe}_{24}\text{Cr}_5\text{N}_y$  at 293 K.

0.87 T and 104.8  $\text{kJ}/\text{m}^3$ , respectively. Similar hard magnetic properties were observed for the carbide powder [12].

The dependence of the coercivity  $\mu_{0i}H_c$  (at 293 K) on the magnetizing field for the carbide sample with  $d=0.8$   $\mu\text{m}$  is shown in Fig. 2. It can be seen that with increasing magnetizing field  $\mu_0H_m$ , the coercivity increases linearly

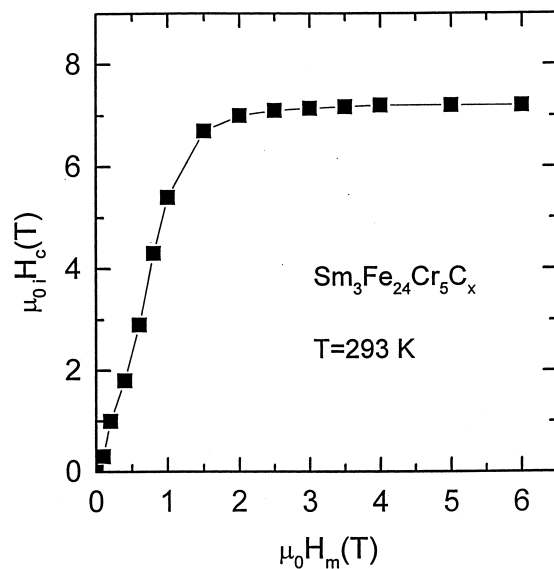


Fig. 2. Magnetizing field dependence of the coercivity  $\mu_{0i}H_c$  with average particle size  $d=0.8$   $\mu\text{m}$  of  $\text{Sm}_3\text{Fe}_{24}\text{Cr}_5\text{C}_x$  at 293 K.

for  $\mu_0 H_m < 1$  T then increases slowly for  $1 \text{ T} < \mu_0 H_m < 2$  T, finally saturating for  $\mu_0 H_m > 2$  T. The maximum coercivity is 0.72 T. For a carbide sample with  $d=0.5 \mu\text{m}$  the maximum coercivity is 0.80 T [11]. A similar magnetizing field dependence of the coercivity for nitride samples with  $d=1.6 \mu\text{m}$  and  $0.6 \mu\text{m}$  was also observed [10]. It can be seen from Fig. 2 that the magnetizing field dependence of the coercivity is smooth and the saturating magnetizing field needed to obtain the highest coercivity is quite low. These results suggest that the coercivity of the carbide and nitride powders is mainly controlled by a nucleation mechanism as observed in  $\text{Sm}_3(\text{Fe,Ti})_{29}\text{N}_y$  and  $\text{Sm}_3(\text{Fe,Cr})_{29}\text{N}_y$  nitrides [10,16] and 2:17:N nitrides [17].

### 3.2. Temperature dependence

Hysteresis loops of a cylindrical carbide  $\text{Sm}_3\text{Fe}_{24}\text{Cr}_5\text{C}_y$  sample with  $d=0.8 \mu\text{m}$  were measured in the temperature range 4.2–450 K. Values of the remanence  $B_r$  and intrinsic coercivity  $\mu_{0i}H_c$  at different temperatures were deduced from the hysteresis loops. The temperature dependencies of  $B_r$  and  $\mu_{0i}H_c$  for the carbide sample with  $d=0.8 \mu\text{m}$  are shown in Fig. 3. The thermal variations of the saturation magnetization  $J_s$  and anisotropy field  $B_a$  of the carbide are also given in Fig. 3 for comparison. The temperature dependencies of  $B_r$  and  $J_s$  are similar but the temperature dependencies of  $\mu_{0i}H_c$  and  $B_a$  are clearly different, with the coercivity decreasing much faster than the anisotropy field.

In order to investigate the temperature stability of the

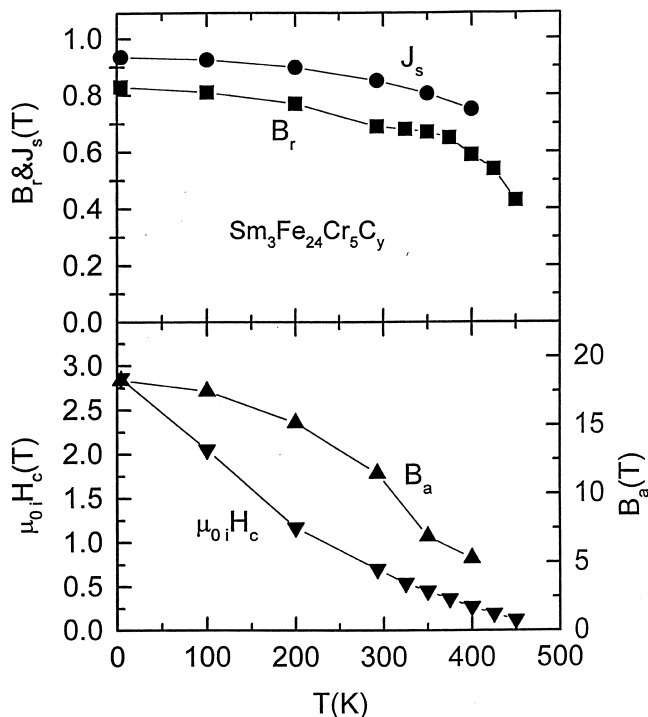


Fig. 3. The temperature dependence of  $B_r$ ,  $\mu_{0i}H_c$ ,  $J_s$  and  $H_a$  for  $\text{Sm}_3\text{Fe}_{24}\text{Cr}_5\text{C}_y$  sample with  $d=0.8 \mu\text{m}$  from 4.2–450 K.

3:29-type carbides, the temperature coefficients of the remanence and the coercivity were calculated from the slopes of the corresponding curves shown in Fig. 3. The remanence and coercivity temperature coefficients at a temperature  $T$  are defined as [18]:

$$\alpha_T = \lim_{\Delta T \rightarrow 0} [B_r(T + \Delta T) - B_r(T)] / B_r(T) / \Delta T * 100 [\% / \text{K}]$$

and

$$\beta_T = \lim_{\Delta T \rightarrow 0} [\mu_{0i}H_c(T + \Delta T) - \mu_{0i}H_c(T)] / \mu_{0i}H_c(T) / \Delta T * 100 [\% / \text{K}].$$

The temperature coefficients of  $B_r$  and  $\mu_{0i}H_c$  for the  $\text{Sm}_3\text{Fe}_{24}\text{Cr}_5\text{C}_y$  sample with  $d=0.8 \mu\text{m}$  are plotted in Fig. 4, along with data for commercial NEOMAX-35 (Nd–Fe–B) [18]. The temperature coefficient of the coercivity for  $\text{Sm}_3\text{Fe}_{24}\text{Cr}_5\text{C}_y$  is better than that of NEOMAX-35 in the temperature range investigated whereas the temperature coefficient of the remanence is not as good as that of NEOMAX-35, especially above about 375 K. Although the Curie temperature ( $T_c=559$  K) of the  $\text{Sm}_3\text{Fe}_{24}\text{Cr}_5\text{C}_y$  carbide is virtually the same as that of NEOMAX-35 ( $T_c=558$  K), the coercivities of the  $\text{Sm}_3\text{Fe}_{24}\text{Cr}_5\text{C}_y$  samples are clearly lower than that of NEOMAX-35. The increase in the absolute value of the temperature coefficient of remanence for the  $\text{Sm}_3\text{Fe}_{24}\text{Cr}_5\text{C}_y$  sample at high temperature results from the faster decrease of the remanence.

### 3.3. Corrosion resistance

Powders of  $\text{Sm}_3\text{Fe}_{24}\text{Cr}_5\text{C}_y$ ,  $\text{Sm}_3\text{Fe}_{24}\text{Cr}_5\text{N}_y$  and sintered Nd–Fe–B magnet phase with average particle sizes of

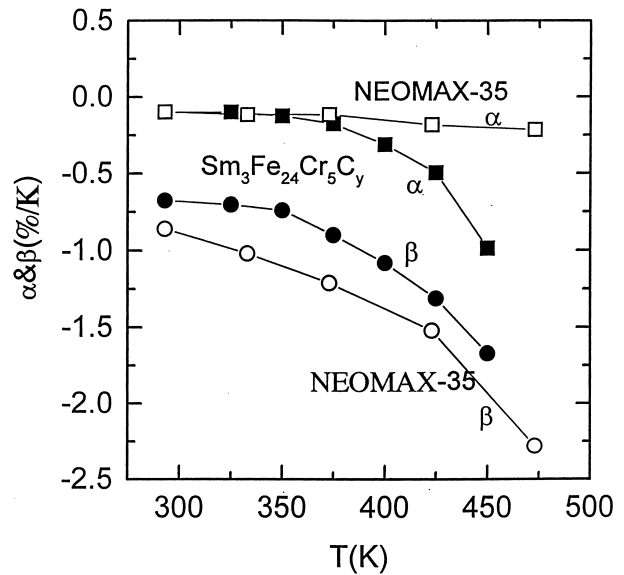


Fig. 4. Thermal variation of the temperature coefficients of the remanence and coercivity for  $\text{Sm}_3\text{Fe}_{24}\text{Cr}_5\text{C}_y$  and NEOMAX-35 magnet phase [18] from 293 K to 450 K.

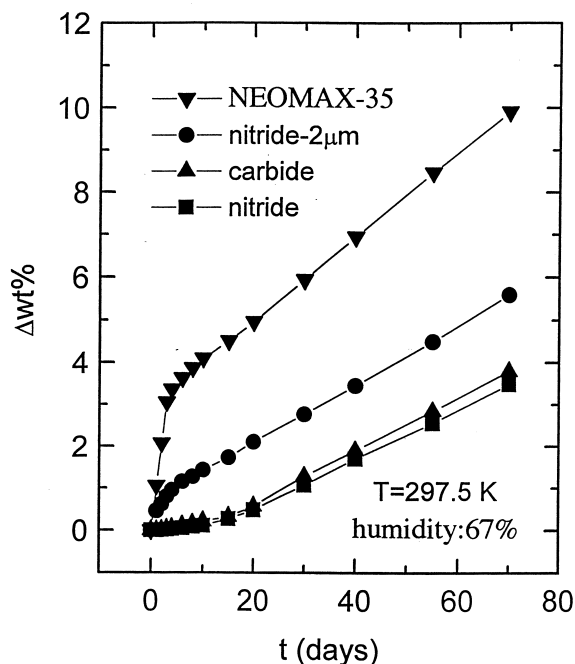


Fig. 5. Weight changes of  $\text{Sm}_3\text{Fe}_{24}\text{Cr}_5\text{C}_y$ ,  $\text{Sm}_3\text{Fe}_{24}\text{Cr}_5\text{N}_y$  and Nd–Fe–B powders with exposure time in a humid environment at 297.5 K.

20–35  $\mu\text{m}$  were placed together in a closed container with a constant relative humidity of 87%, created using a saturated aqueous solution of an excess of  $\text{Na}_2\text{CO}_3 \cdot 10\text{H}_2\text{O}$ , at 297.5 K for 70 days. The weight change of the samples was monitored during the examination. Each powder was put in a glass container and all the containers were dried in air for 20–30 min before weighing. Fig. 5 shows the time-evolution of the weight changes of the powder samples of  $\text{Sm}_3\text{Fe}_{24}\text{Cr}_5\text{C}_y$ ,  $\text{Sm}_3\text{Fe}_{24}\text{Cr}_5\text{N}_y$  and sintered Nd–Fe–B. From Fig. 5 we can clearly see that the weight increases for the 3:29 nitride and carbide powders are lower than that of Nd–Fe–B powder, indicating that the nitride and carbide have better corrosion resistance than Nd–Fe–B, under these conditions. We can also see that the rate of corrosion becomes almost the same for all the powders after about 3 weeks and only in the initial few days is the corrosion of the Nd–Fe–B powder and  $\text{Sm}_3\text{Fe}_{24}\text{Cr}_5\text{N}_y$  ( $d=2.5 \mu\text{m}$ ) much faster than that of the other samples. This indicates that there is a large difference in the corrosion resistance at the initial stage of the oxidization.

#### 4. Conclusion

The extrinsic hard magnetic properties of the  $\text{Sm}_3\text{Fe}_{24}\text{Cr}_5\text{X}_y$  ( $\text{X}=\text{N},\text{C}$ ) compounds have been investigated. An intrinsic coercivity  $\mu_0 H_c$  of 0.80 T at 293 K has

been developed. The temperature coefficient of the remanence for both the 3:29 nitride and carbide samples is worse than that of NEOMAX-35, but the temperature coefficient of the coercivity is better. The  $\text{Sm}_3\text{Fe}_{24}\text{Cr}_5\text{X}_y$  nitride and carbide powders have better corrosion resistance than Nd–Fe–B powder. Our results suggest that both 3:29 carbides and nitrides are suitable as a main phase for high performance permanent magnet applications.

#### Acknowledgements

This work was partly supported by the National Natural Science Foundation of China and the Bilateral Science and Technology Collaboration Programme sponsored by the Department of Industry, Science and Technology, Australia.

#### References

- [1] Y.V. Shcherbakova, G.V. Ivanova, A.S. Yermolenko, Y.V. Belozarov, V.S. Gaviko, *J. Alloys Compounds* 182 (1992) 119.
- [2] S.J. Collocott, R.K. Day, J.B. Dunlop, R.L. Davis, Proc. 7th Int. Symp. on Magnetic Anisotropy and Coercivity in Rare-Earth Transition Metal Alloys, Canberra, 1992, pp. 437.
- [3] H.S. Li, J.M. Cadogan, R.L. Davis, A. Margarian, J.B. Dunlop, *Solid State Commun.* 90 (1994) 487.
- [4] Z. Hu, W.B. Yelon, *Solid State Commun.* 91 (1994) 223.
- [5] F.M. Yang, B. Nasunjilegal, J.L. Wang, H.Y. Pan, W.D. Qing, R.W. Zhao, B.P. Hu, Y.Z. Wang, G.C. Liu, H.S. Li, J.M. Cadogan, *J. Appl. Phys.* 76 (1994) 1971.
- [6] B.P. Hu, G.C. Liu, Y.Z. Wang, B. Nasunjilegal, N. Tang, F.M. Yang, H.S. Li, J.M. Cadogan, *J. Phys. Condens. Matter* 6 (1994) L595.
- [7] X.F. Han, F.M. Yang, Q.S. Li, M.C. Zhang, S.Z. Zhou, *J. Phys. Condens. Matter.* (submitted).
- [8] Y.Z. Wang, H.S. Li, X.F. Han, G.C. Liu, B.P. Hu, C.P. Yang, N. Tang, F.M. Yang, *J. Alloys Compounds* 260 (1997) 277.
- [9] B.P. Hu, G.C. Liu, Y.Z. Wang, B. Nasunjilegal, R.W. Zhao, F.M. Yang, H.S. Li, J.M. Cadogan, *J. Phys. Condens. Mat.* 6 (1994) L197.
- [10] Y.Z. Wang, G.C. Liu, B.P. Hu, H.S. Li, X.F. Han, C.P. Yang, *J. Phys. Condens. Mat.* 9 (1997) 2787.
- [11] Y.Z. Wang, G.C. Liu, B.P. Hu, H.S. Li, X.F. Han, C.P. Yang, *J. Phys. Condens. Mat.* 9 (1997) 2793.
- [12] X.F. Han, M.C. Zhang, Y. Qiao, F.M. Yang, Y.Z. Wang, *J. Magn. Magn. Mater.* (submitted).
- [13] X.F. Han, Y.Z. Wang, M.C. Zhang, F.M. Yang, G.C. Liu, C.P. Yang, B.P. Hu, *J. Alloy Compounds* (submitted).
- [14] H.G. Pan, F.M. Yang, Y. Chen, X.F. Han, N. Tang, C.P. Chen, Q.D. Wang, *J. Phys. Condens. Mat.* 9 (1997) 2499.
- [15] F.E. Luborsky, *J. Appl. Phys.* 32 (1961) 171S.
- [16] J.F. Hu, F.M. Yang, B. Nasunjilegal, R.W. Zhao, H.Y. Pan, Z.X. Wang, B.P. Hu, Y.Z. Wang, G.C. Liu, *J. Phys. Condens. Mat.* 6 (1994) L411.
- [17] B.P. Hu, X.L. Rao, J.M. Xu, G.C. Liu, Y.Z. Wang, X.L. Dong, D.X. Zhang, M. Cai, *J. Appl. Phys.* 74 (1993) 489.
- [18] D. Li, H.F. Mildrum, K.J. Strnat, *J. Appl. Phys.* 57 (1985) 140.